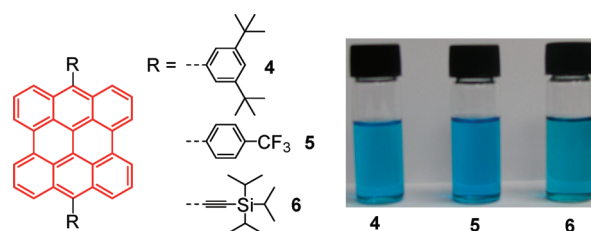# *meso*-Substituted Bisanthenes as Soluble and Stable Near-infrared Dyes

Jinling Li,[†] Kai Zhang,[†] Xiaojie Zhang,[†] Kuo-Wei Huang,[‡] Chunyan Chi,[†] and Jishan Wu*,[†]

[†]*Department of Chemistry, National University of Singapore, 3 Science Drive 3, Singapore 117543 and* [‡]*KAUST Catalysis Center and Division of Chemical and Life Sciences and Engineering, 4700 King Abdullah University of Science and Technology, Thuwal 23955-6900, Kingdom of Saudi Arabia*

chmwuj@nus.edu.sg

Three *meso*-substituted bisanthenes, **4**−**6**, were prepared in a short synthetic route from the bisanthenequinone. They exhibit largely improved stability and solubility in comparison to the parent bisanthene. All of these compounds also show near-infrared (NIR) absorption and emission with high to moderate fluorescence quantum yields. Amphoteric redox behavior was observed for **4**−**6** by cyclic voltammetry, and these compounds can be reversibly oxidized and reduced into respective cationic and anionic species by both electrochemical and chemical processes. In addition, compound **5** adopts a herringbone π-stacking motif in the single crystal.

Introduction

Near infrared (NIR) dyes[1] with absorption and/or emission in the spectral range of 700−1400 nm are of importance for many potential applications such as high-contrast bioimaging,[2] optical recording,[3] NIR laser filter,[4] NIR photography,[5] solar cells,[6] and optical limiting at telecommunications wavelength.[7]

However, many commercially available NIR dyes such as cyanine dyes suffer from inevitable drawbacks due to their insufficient photostability.[8]

Polycyclic aromatic hydrocarbons (PAHs) usually exhibit excellent chemical stability and photostability with respect to the traditional cyanine dyes, and one good example is rylene (oligo-*peri*-naphthalene), which is a type of important stable dye/pigment used in industry.[9] For the design of PAH-based NIR dyes, largely extended π-conjugation is usually required. For example, the alkyl- or carboximide-substituted rylene molecules show NIR absorption only when the molecular length reaches four naphthalene units (quaterrylene).[10]

(1) (a) Fabian, J.; Nakanzumi, H.; Matsuoka, M. *Chem. Rev.* **1992**, *92*, 1197–1226. (b) Fabian, J.; Zahradnik, R. *Angew. Chem., Int. Ed. Engl.* **1989**, *28*, 677–828.

(2) (a) Kiyose, K.; Kojima, H.; Nagano, T. *Chem. Asian J.* **2008**, *3*, 506–515. (b) Amiot, C. L.; Xu, S. P.; Liang, S.; Pan, L. Y.; Zhao, X. J. *Sensors* **2008**, *8*, 3082–3105.

(3) Emmelius, M.; Pawlowski, G.; Vollmann, H. W. *Angew. Chem., Int. Ed. Engl.* **1989**, *28*, 1445–1470.

(4) Kololuoma, T.; Oksanen, J. A. I.; Raerinne, P.; Rantala, J. T. *J. Mater. Res.* **2001**, *16*, 2186–2188.

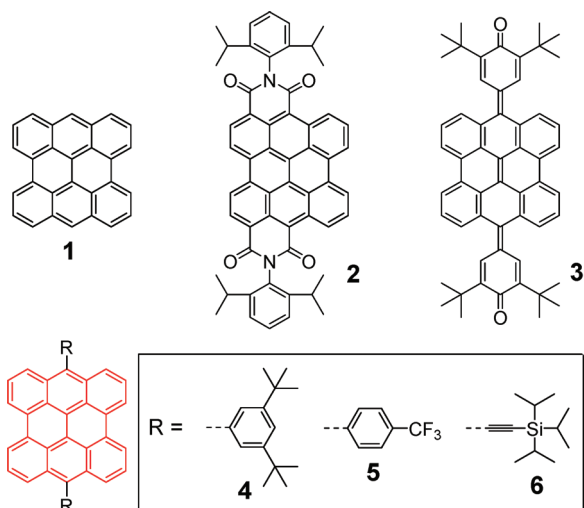(5) Tani, T.; Kikuchi, S. *Photogr. Sci. Eng.* **1967**, *11*, 129–144.

(6) (a) Imahori, H.; Umeyama, T.; Ito, S. *Acc. Chem. Res.* **2009**, *42*, 1809–1818. (b) Reddy, P. Y.; Gribabu, L.; Lyness, C.; Snaith, H. J.; Vijaykumar, C.; Chandrasekharam, M.; Lakshmikantam, M.; Yum, J.-H.; Kalyanasundaram, K.; Grätzel, M.; Nazeeruddin, M. K. *Angew. Chem., Int. Ed.* **2007**, *46*, 373–376.

(7) (a) Beverina, L.; Fu, J.; Leclercq, A.; Zojer, E.; Pacher, P.; Barlow, S.; Van Stryland, E. W.; Hagan, D. J.; Brédas, J. -L.; Marder, S. R. *J. Am. Chem. Soc.* **2005**, *127*, 7282–7283. (b) Bouit, P. A.; Wetzel, G.; Berginc, G.; Loiseaux, B.; Toupet, L.; Feneyrou, P.; Bretonnière, Y.; Kamada, K.; Maury, O.; Andraud, C. *Chem. Mater.* **2007**, *19*, 5325–5335.

(8) Gregory, P. *High-Technology Applications of Organic Colorants*; Plenum: New York, 1991.

(9) (a) Herrmann, A.; Müllen, K. *Chem. Lett.* **2006**, *35*, 978–985. (b) Pschirer, N. G.; Kohl, C.; Nolde, F.; Qu, J.; Müllen, K. *Angew. Chem., Int. Ed.* **2006**, *45*, 1401–1404. (c) Sinks, L. E.; Rybtchinski, B.; Iimura, M.; Jones, B. A.; Goshe, A. J.; Zuo, X. B.; Tiede, D. M.; Li, X.-Y.; Wasielewski, M. R. *Chem. Mater.* **2005**, *17*, 6295–6303. (d) Hortrup, F. O.; Müller, G. R. J.; Quante, H.; de Feyter, S.; de Schryver, F. C.; Müllen, K. *Chem.—Eur. J.* **1997**, *3*, 219–225.

(10) (a) Quante, H.; Müllen, K. *Angew. Chem., Int. Ed. Engl.* **1995**, *34*, 1323–1325. (b) Geerts, Y.; Quante, H.; Platz, H.; Mahrt, R.; Hopmeier, M.; Böhm, A.; Müllen, K. *J. Mater. Chem.* **1998**, *8*, 2357–2369. (c) Langhals, H.; Büttner, J.; Blanke, P. *Synthesis* **2005**, 364–366. (d) Jiao, C. J.; Huang, K. W.; Luo, J.; Zhang, K.; Chi, C. Y.; Wu, J. *Org. Lett.* **2009**, *11*, 4508–4511.

CHART 1. **Molecular Structures of Bisanthene 1 and Its Derivatives 2−6**

FIGURE 1. Normalized UV−vis−NIR absorption and photoluminescence spectra of compounds **4**, **5**, and **6**. The concentrations for the absorption and emission spectroscopic measurements in toluene are 10^{-5} and 10^{-6} M, respectively.

SCHEME 1. **Synthetic Route to *meso*-Substituted Bisanthenes 4−6**

Moreover, previous research disclosed that the band gap of a PAH molecule depended on not only the molecular size but also the edge structure.[11] The arm-chair edged PAHs usually exhibit high chemical stability but a large band gap. On the other hand, theoretical calculations suggested that zigzag edged PAH molecules with a smaller benzenoid component would show low band gap with near-infrared absorption.[12] Our recent interest is a type of zigzag edged, *peri*-fused oligoacenes, namely, *periacenes*, which are expected to exhibit NIR absorption and emission.[12] As the smallest member of the periacene family, bisanthene (**1**, Chart 1) was reported to show far-red absorption with absorption maximum at 662 nm.[13] However, the parent bisanthene is a very unstable compound and decomposes quickly in solution under ambient air and light condition. This is mainly because of its highlying HOMO level, and it is ready to undergo addition reaction with the singlet oxygen in air.[13] Like the zigzag edged pentacene compound,[11b] the reactive sites in bisanthene are the *meso*-positions of the zigzag edges. We recently found that attachment of two electron-withdrawing dicarboxylic imide groups at the zigzag edges of the bisanthene (compound **2** in Chart 1) not only largely improved its stability but also significantly shifted the absorption to the NIR spectral range with the absorption maximum at 830 nm.[14] In addition, quinoidal bisanthene **3** (Chart 1) was also prepared and exhibited good stability with NIR absorption.[15] While these methods are successful, we are looking for an alternative approach to prepare soluble and stable bisanthene-based NIR dyes by a short synthetic route. Herein, we report that substitution at the active *meso*-positions of the
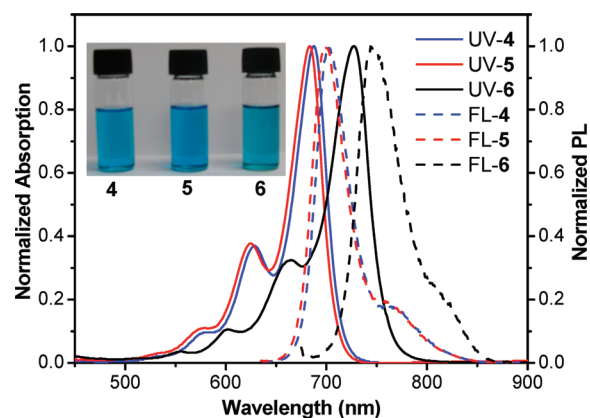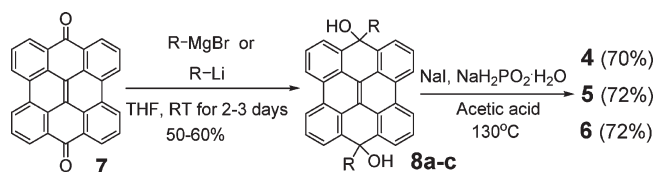
bisanthene with either aryl or alkyne group is also an efficient way to achieve our target. In this work, two aryl-substituted bisanthenes, **4** and **5**, and one triisopropylsilylethynyl-substituted bisanthene, **6** (Chart 1), were prepared. The substituents are chosen on the basis of several considerations: (a) Conjugation effect. The aryl and alkyne groups are supposed to at least partially extend the π-conjugation with the central bisanthene units so that the absorption and emission spectral can shift into NIR spectral range. At the same time, the extended π-conjugation can also improve the stability of the electron-rich bisanthene unit by extended electron delocalization. (b) Steric effect. The bulky substitution at the *meso*-positions can prevent the oxidative addition of singlet oxygen to the bisanthene core. Meanwhile, the solubility can be also improved as a result of diminished intermolecular interactions (especially for compound **4**). (c) Electronic effect. To form stable bisanthene derivatives, electron-withdrawing groups should be attached. Herein, three substituents with different electron-donating/-accepting capabilities are introduced; in particular, the trifluoromethylphenyl in compound **5** and the triisopropylsilylethynyl groups in **6** are both electron-withdrawing groups that are expected to enhance the stability of the electron rich bisanthene. The photophysical properties and electrochemical behavior of compounds **4−6** were studied, and the effect of the different substituents on their properties is discussed in detail. In addition, geometric structure and molecular packing of one of these compounds was studied by crystallographic analysis, and their potential as semiconductors in a field effect transistor (FET) is also discussed.

Results and Discussions

Synthesis. The synthesis of compounds **4**, **5**, and **6** is depicted in Scheme 1. Bisanthenequinone **7** was first

(11) (a) Wu, J.; Pisula, W.; Müllen, K. *Chem. Rev.* **2007**, *107*, 718−747. (b) Anthony, J. E. *Angew. Chem., Int. Ed.* **2008**, *47*, 452−483.

(12) (a) Jiang, D. E.; Sumpter, B. G.; Dai, S. *J. Chem. Phys.* **2007**, *127*, 124703. (b) Jiang, D. E.; Dai, S. *Chem. Phys. Lett.* **2008**, *466*, 72−75. (c) Jiang, D. E.; Dai, S. *J. Phys. Chem. A* **2008**, *112*, 332−335. (d) Chen, Z. F.; Jiang, D. E.; Lu, X.; Bettinger, H. F.; Dai, S.; von Ragué, Schleyer, P.; Houk, K. N. *Org. Lett.* **2007**, *9*, 5449−5452.

(13) (a) Arabei, S. M.; Pavich, T. A. *J. Appl. Spectrosc.* **2000**, *67*, 236−244. (b) Kuroda, H. *J. Chem. Soc.* **1960**, 1856−1857. (c) Clar, E. *Chem. Ber.* **1948**, *81*, 52−63.

(14) Yao, J.; Chi, C.; Wu, J.; Loh, K. *Chem.—Eur. J.* **2009**, *15*, 9299−9302.

(15) Zhang, K.; Huang, K. W.; Li, J. L.; Luo, J.; Chi, C. Y.; Wu, J. *Org. Lett.* **2009**, *11*, 4854−4857.

TABLE 1. Summary of Photophysical and Electrochemical Properties of Compounds 4, 5, and 6[a]

compounds	λ_{abs} (nm)			ε_{max} (M^{-1} cm^{-1})	λ_{em} (nm)	QY (nm)	E_{ox}^1 (V)	E_{ox}^2 (V)	E_{ox}^3 (V)	E_{red}^1 (V)	E_{red}^2 (V)	HOMO (eV)	LUMO (eV)	E_g^{opt} (eV)
4	687	628	582	38 438	701	0.81	0.44	1.03		−1.21	−1.65	−4.71	−3.20	1.73
5	683	624	580	45 098	699	0.80	0.53	1.14		−1.10	−1.53	−4.80	−3.31	1.74
6	727	662	603	55 690	744	0.38	0.34	0.72	1.20	−0.92	−1.31	−4.57	−3.47	1.62

[a] E_{ox}^n and E_{red}^n are half-wave potentials for respective redox waves with AgCl/Ag as reference. HOMO and LUMO energy levels were calculated from the onset potentials of the first oxidation (E_{ox}^{onset}) and the first reduction wave (E_{red}^{onset}) according to the following equations: HOMO = −(4.8 + E_{ox}^{onset}) and LUMO = −(4.8 + E_{red}^{onset}), where the potentials are referred to $E_{Fc+/Fc}$.
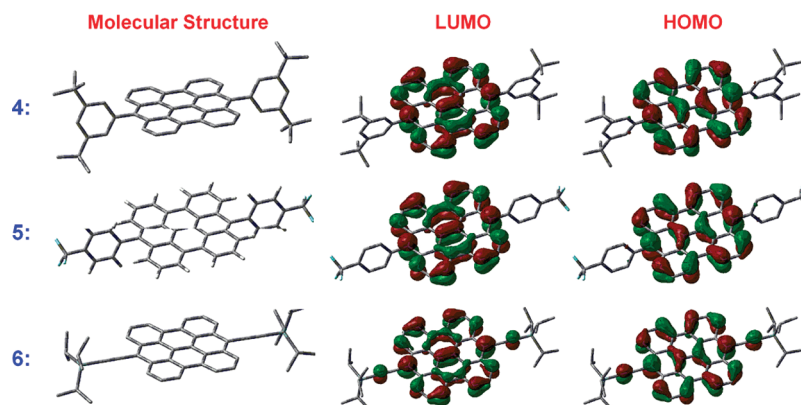

FIGURE 2. Optimized structure and frontier molecular orbital profiles of molecules 4−6 based on DFT (B3LYP/6-31G**) calculations.

prepared in gram scale according to literature procedure.[13] The subsequent chemistry is similar to that of pentacenequinone.[16] Compound 7 reacted with the Grignard reagent of the respective arenes or the lithium reagent of triisopropylsilylacetylene in anhydrous THF to give the respective alcohols 8a−c in 50−60% yields. This was followed by dehydroxylation and reductive aromatization with NaI/NaH$_2$PO$_2$ to afford the target compounds 4, 5, and 6 in good yields. Actually, this two-step reaction can also be done in one pot without separation of the intermediate compound 8a−c. Thus this synthetic route is obviously simple and straightforward, and the target compounds can be obtained by simple column chromatography purification. Compounds 4−6 have good solubility in normal organic solvents such as chloroform and THF; in particular, the 3,5-di-tert-butylphenyl-substituted bisanthene 4 shows the highest solubility due to the very bulky substitution. All of the intermediate compounds and the final products are well characterized by NMR spectroscopy and high resolution mass spectrometry (see Supporting Information).

Photophysical Properties and Theoretical Calculations. The UV−vis−NIR absorption and fluorescence spectra of 4, 5, and 6 recorded in toluene are shown in Figure 1, and the data are collected in Table 1. Solutions of 4−6 in toluene display a blue color and well-resolved absorption bands between 500 and 800 nm with the maximum peak at 687 (molar extinction coefficient ε = 38 438 M^{-1} cm^{-1}), 683 (ε = 45 098 M^{-1} cm^{-1}), and 727 (ε = 55 690 M^{-1} cm^{-1}) nm,

respectively. Compared with the absorption spectra of bisanthene,[13] there is a red-shift of about 25, 21, and 65 nm for 4, 5, and 6, respectively. The red-shift for all of these compounds indicates that π-conjugation of the bisanthene core is further extended by incorporation of the aryl and triisopropylsilylethynyl moieties. DFT (B3LYP/6-31G**) calculations of 4−6 were then conducted to further understand their geometric and electronic structures. The optimized structure and the frontier molecular orbital profiles of 4−6 are shown in Figure 2. The phenyl moieties in 4 and 5 are twisted about 80° with respect to the bisanthene plane, and as a result, only weak electron delocalization between the phenyl ring and the bisanthene units was observed for 4 and 5. However, for 6, obvious electron delocalization between the ethynyl moiety and the bisanthene unit was observed. Such a structural difference accounts for the difference in their absorption spectra where the largest red-shift was found for 6. In addition, time-dependent DFT calculations also predict that the absorption maxima for 4−6 are 716.3, 714.4, and 785.6 nm, respectively, and such tendency also agrees well with our experimental results.

Compounds 4−6 also show strong fluorescence with the emission maximum at 701, 699, and 744 nm, respectively (Figure 1 and Table 1). Their photoluminescence quantum yields (Φ) were determined according to an optical dilute method (optical density A < 0.05) by using cardiogreen dye (λ_{abs} (max) = 780 nm, Φ = 0.13 in DMSO) as a standard.[17] The Φ values of 0.81, 0.80, and 0.38 were obtained for 4, 5, and 6, respectively. Such high to moderate quantum yields for NIR dye are remarkable given that many NIR absorbing

(16) (a) Allen, C. F. H.; Bell, A. J. Am. Chem. Soc. 1942, 64, 1253–1261. (b) Funk, R. L.; Young, E. R. R.; Williams, R. M.; Flanagan, M. F.; Cecil, T. L. J. Am. Chem. Soc. 1996, 118, 3291–3292. (c) Miller, G. P.; Mack, J.; Briggs, J. Org. Lett. 2000, 2, 3983–3286. (d) Anthony, J. E.; Eaton, D. L.; Parkin, S. R. Org. Lett. 2002, 4, 15–18. (e) Jiang, J. Y.; Kaafarani, B. R.; Neckers, D. C. J. Org. Chem. 2006, 71, 2155–2158. (f) Wudl, F.; Perepichka, D. F. Chem. Rev. 2004, 104, 4891–4945.

(17) Licha, K.; Riefke, B.; Ntziachristos, V.; Becker, A.; Chance, B.; Semmler, W. Photochem. Photobiol. 2000, 72, 392–398.
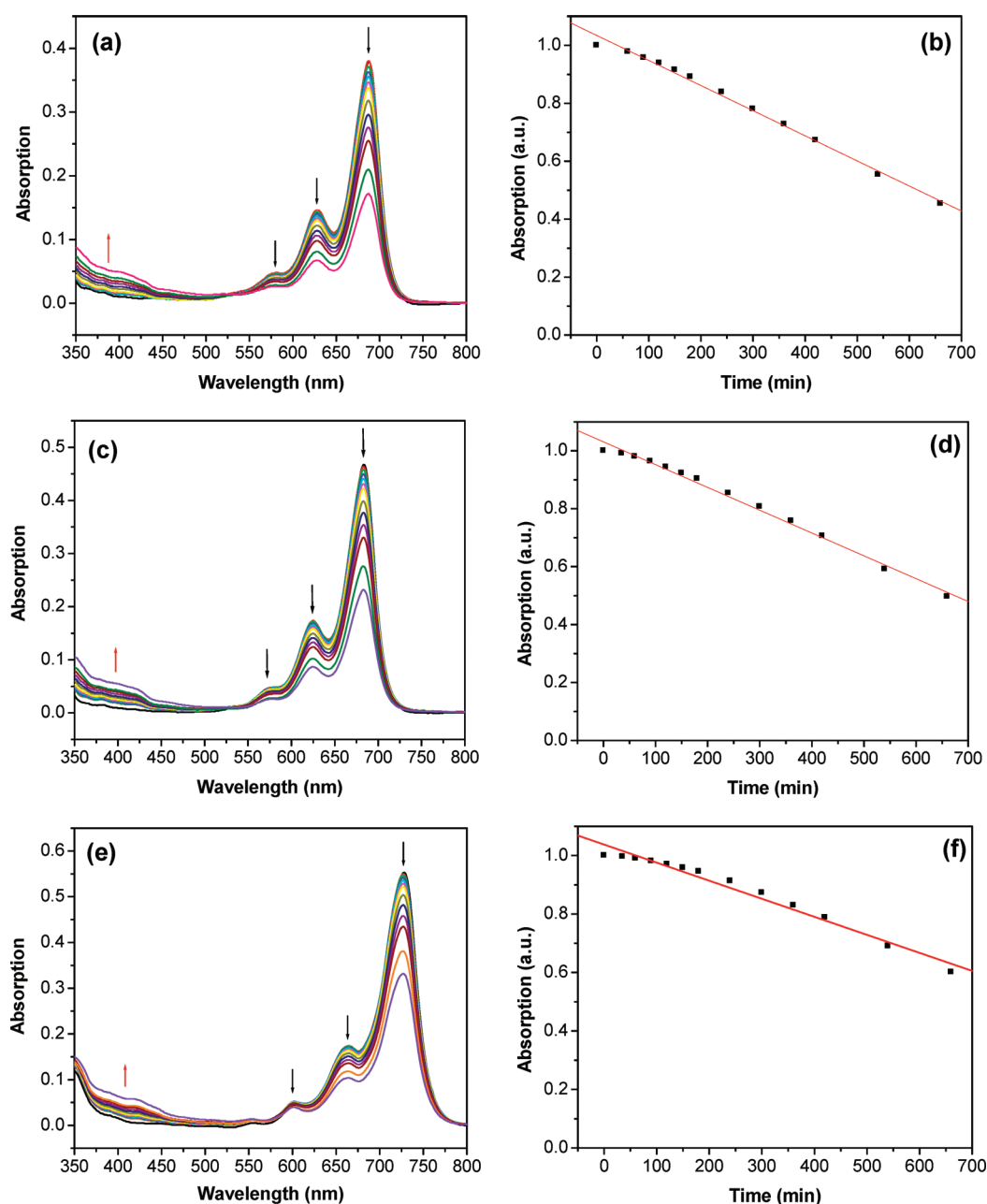
FIGURE 3. Photostability test of compounds **4**−**6** in toluene upon irradiation by 100 W white light bulb. (Left) UV−vis−IR absorption spectra of **4** (a), **5** (c), and **6** (e) in toluene recorded during the irradiation. The arrows indicate the change in the spectra. (Right) Change of optical density of **4** (b), **5** (d), and **6** (f) at the absorption maximum wavelength with the irradiation time. The original optical density before irradiation was normalized at the absorption maximum.

dyes (including the bisanthenes **1**−**3**) usually exhibit low fluorescence quantum yields.

Photostability and Thermal Stability. In contrast to the very unstable parent bisanthene, the air-saturated solutions of **4**, **5**, and **6** in toluene are stable for weeks under ambient conditions without significant change on their UV−vis−NIR absorption spectra. Upon irradiation of white light (100 W), the solutions gradually decomposed with a decrease of the optical intensity at the major absorption band (550−800 nm) and appearance of new absorption band in the shorter wavelength (Figure 3). The half-times ($t_{1/2}$) of around 618, 674, and 870 min were estimated for **4**, **5**, and **6**, respectively, by plotting the optical density at the absorption

maximum with the irradiation time (Figure 3). Upon irradiation by UV lamp (4 W), the decomposition process became faster, and the compounds displayed $t_{1/2}$ of about 404, 452, and 586 min, respectively (Figure S1 in Supporting Information). These results revealed that the photostability of the bisanthene-based compounds followed the sequence **6** > **5** > **4** ≫ **1** and also proved that introduction of phenyl or triisopropylsilylethynyl groups at the *meso*-positions of the bisanthene unit largely improved the stability of the chromophore. The difference in the stability of the bisanthene **1** and its derivatives **4**−**6** can be explained by a combination of the electronic effect, conjugation effect, and steric effect of the substituents. Without any substituent, the parent

bisanthene **1** with a high lying HOMO energy level can be easily oxidized by adding singlet oxygen to the core, and eventually a more stable bisanthenequinone **7** is formed.[13] However, after substitution by aryl and alkyne at the *meso*-positions, the bulky substituents significantly prohibit the intermolecular interaction between the oxygen and the bisanthene core. Moreover, the extended π-conjugation between the bisanthene and the aryl or alkyne moieties further delocalizes the electron cloud and leads to a more stable extended π-system; in particular, the electron delocalization is more effective in **6** with respect to **4** and **5**. Moreover, electron-withdrawing effect also plays an important role in the stability of the bisanthene chromophore. For **5**, the electron-withdrawing trifluoromethyl group on the phenyl ring reduces the electron density of the bisanthene backbone, so it is less photo-oxidizable than **4**. For **6**, the ethynyl group is fully conjugated to the bisanthene π-system (resonance effect) and the sp-hybridized ethynyl carbons are modestly more electronegative than sp^2-hybridized carbons to which they are attached (inductive effect), so compound **6** is most stable. Such a trend is also in agreement with the observation for *meso*-substituted pentacene derivatives.[18]

Thermogravimetric analysis (TGA) measurements reveal that **4** and **5** are highly stable with a decomposition temperature of about 410 °C (5 wt % weight loss) in N_2 atmosphere, whereas for compound **6**, its decomposition temperature is about 334 °C, probably because of the relatively poor thermal stability of C≡C units (Figure S2 in Supporting Information). For these three compounds, neither glass transition nor crystal melting point or liquid crystalline-isotropic transition was observed in the temperature range of 25−300 °C by means of differential scanning calorimetry (DSC). So we can conclude that after substitution at the *meso*-positions of bisanthene, new soluble and stable near-infrared absorbing and emitting dyes **4−6** are obtained.

Electrochemical Properties and Chemical Oxidation Titration. The electrochemical properties of compounds **4−6** were investigated by cyclic voltammetry (CV) in dry DCM (Figure 4), and the data are collected in Table 1. The cyclic voltammograms of **4** and **5** exhibit two reversible oxidation waves with half-wave potentials (E_{ox}^n) at 0.44 and 1.03 V for **4** and 0.53 and 1.14 V for **5**, while three oxidative waves were observed for **6**, with E_{ox}^n at 0.34, 0.72, and 1.20 V (vs AgCl/Ag). Compounds **4**, **5**, and **6** also show two quasi-reversible reduction waves with the half-wave potential of the first reductive waves (E_{red}^1) at −1.21, −1.10, and −0.92 V, respectively. Such an amphoteric redox behavior suggests that all of these compounds can be reversibly oxidized into respective cationic species (e.g., radical cations and dications) and reduced into corresponding anionic species (e.g., radical anion and dianion) and the charged species can be stabilized by the largely delocalized π-system. The lowest first oxidation potential observed for **6** can be explained by the most effective π-conjugation between the bisanthene and the ethynyl moieties as we discussed above. Moreover, more detectable oxidation states can be determined for **6**. The first oxidation potential of **5** is higher than that for **4** as a result of
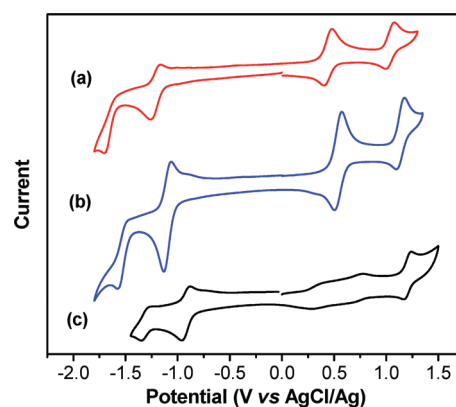

FIGURE 4. Cyclic voltammograms of **4** (a), **5** (b), and **6** (c) in dichloromethane (1 mM) with 0.1 M Bu_4NPF_6 as supporting electrolyte, AgCl/Ag as reference electrode, Au disk as working electrode, Pt wire as counter electrode, and scan rate at 50 mV/s.

the electron-withdrawing effect of the trifluoromethyl groups.

Chemical oxidation titrations of compounds **4−6** were conducted in DCM by using either iodine or $SbCl_5$ as oxidant, and the process was followed by UV−vis−NIR absorption spectroscopy. All of these compounds can be reversibly oxidized by $SbCl_5$ into stable radical cations with the appearance of new characteristic absorption bands in the shorter and longer wavelengths (Figure 5). Such a phenomenon is common due to the redistribution of frontier molecular orbital energy level in the energy gap, and one electron transition at the higher energy and one electron transition at lower energy are allowed in the new energy diagram. The oxidized species can also be reversibly reduced into the neutral state by adding Zn dust to the solution containing oxidized species (Figure 5). Similar reversible process can be observed for **4** and **5** when iodine was used as oxidant. However, chemical oxidization of **5** by iodine is irreversible likely due to electrophilic addition of I^+ onto the C≡C units (Figure S4 in Supporting Information).

The HOMO and LUMO energy levels were deduced from the onset potentials of the first oxidation (E_{ox}^{onset}) and the first reduction wave (E_{red}^{onset}), according to the following equations: HOMO$=-(4.8 + E_{ox}^{onset})$ and LUMO$=-(4.8 + E_{red}^{onset})$, where the potentials are calibrated to $E_{Fc+/Fc}$.[19] Compared with the aryl-substituted bisanthenes (**4** and **5**), compound **6** has a higher lying HOMO energy level (−4.57 eV). However, this compound is still more stable than **4** and **5** because of effective electron delocalization. In agreement with the small optical band gap (E_g^{opt}) determined from the absorption spectra, the electrochemical band gaps are also small due to a convergence of the HOMO and LUMO energy levels. As a result, low band gap materials with NIR absorption and emission are obtained.

Single-Crystal Structure and Molecular Packing. Besides the photophysical and electrochemical properties, molecular structure and solid state packing of these molecules are also of importance when considering of their potential applications as semiconductors in electronic devices such as FET. Single crystal of **5** was successfully obtained by slow

(18) Kaur, I.; Jia, W.-L.; Kopreski, R.-P.; Selvarasah, S.; Dokmeci, M.-R.; Pramanil, C.; McGruer, N.-E.; Miller, G.-P. *J. Am. Chem. Soc.* **2008**, *130*, 16274–16286.

(19) (a) Chi, C.; Wegner, G. *Macromol. Rapid Commun.* **2005**, *26*, 1532–1537. (b) Pommerehne, J.; Vestweber, H.; Guss, W.; Mahrt, R. F.; Bassler, H.; Porsch, M.; Daub, J. *Adv. Mater.* **1995**, *7*, 551–554.
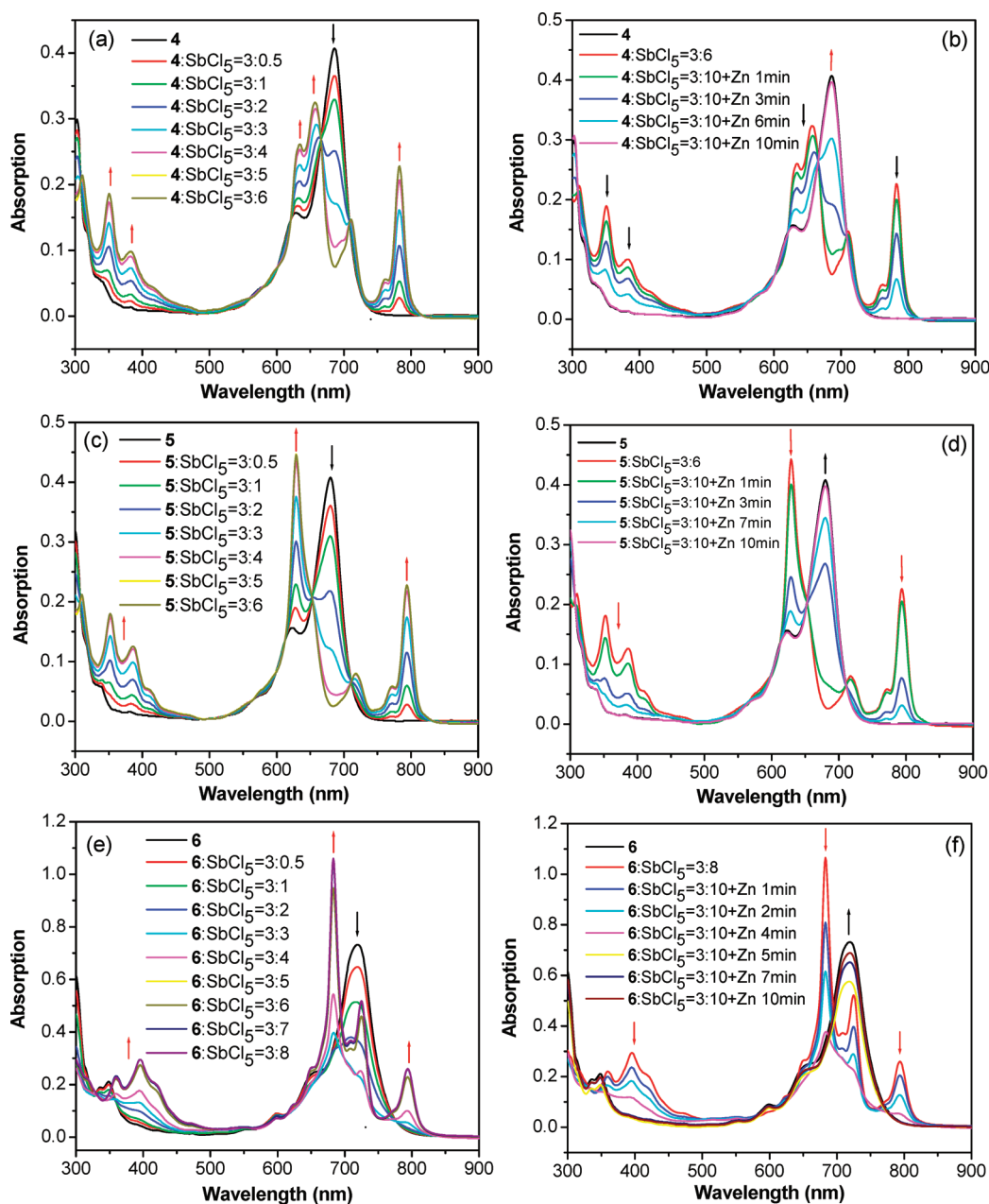
FIGURE 5. (Left) UV−vis−NIR absorption spectra of **4** (a), **5** (c), and **6** (e) during the titration with SbCl$_5$ in dry DCM. The arrows show the changes of the spectra during the titration. (Right) UV−vis−NIR absorption spectra of the oxidized pieces **4** (b), **5** (d), and **6** (f) during reduction by Zn with different contact time. The arrows indicate the changes of the spectra with different contact time with Zn dust.

diffusion of methanol vapor to the chloroform solution. The single-crystal structure and three-dimensional packing of **5** are shown in Figure 6.[20] Compound **5** has a planar bisanthene unit, and the trifluoromethylphenyl groups are twisted from the bisanthene plane by about 80° due to steric congestion (Figure 6a). Such structure is similar to the phenyl-*meso*-substituted pentacene.[16] Interestingly, **5** adopts a layer-like structure (Figure 6b), and in each layer a herringbone π-stacking motif (Figure 6c) was observed. Two types of π−π interactions can be distinguished: an offset π-overlap

between the bisanthene units with a close contact distance of 3.301 Å and an edge-to-face CH-π interaction with a close contact distance of 2.752 Å. Such a close packing mode with strong intermolecular π-interactions suggests that **5** could be a good semiconductor for FET devices.

Conclusions

In summary, three *meso*-substituted bisanthenes **4**−**6** were successfully prepared in a short synthetic route. Compared with the parent bisanthene **1**, compounds **4**−**6** exhibit largely improved stability and solubility. The obtained materials also show bathochromic shift of their absorption and emission spectra into the NIR spectral range with high to moderate fluorescence quantum yields, qualifying them as

(20) Single crystal data for **5**: C$_{42}$H$_{20}$F$_6$, orthorhombic, space group *Pbca*. Unit cell parameters: $a = 10.9112(9)$ Å, $b = 7.7032(7)$ Å, $c = 34.108(3)$ Å, $\alpha = 90°$, $\beta = 90°$, $\gamma = 90°$, volume = 2866.8(4) Å^3, $Z = 4$, density = 1.480 Mg/m^3, $R1 = 0.0775$, $wR2 = 0.1543$.
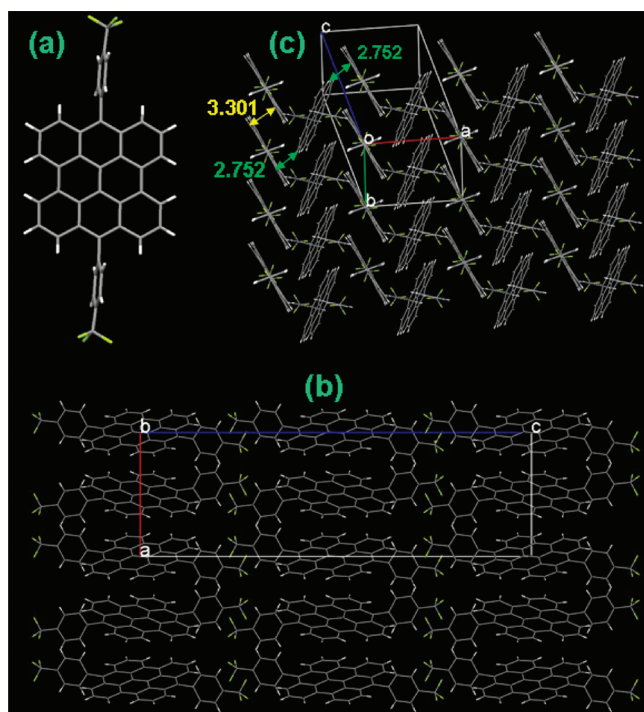
FIGURE 6. Single-crystal structure (a) of compound **5**, its three-dimensional layer-like packing (b), and the herringbone π-stacking motif in each layer (c).

both NIR absorption and fluorescent dyes. These compounds display amphoteric redox behavior with multistep reversible redox processes, suggesting that they could be used as both hole and electron transporting materials. In particular, the ordered herringbone π-stacking mode observed in **5** indicates that it can be used as potential semiconductor in FETs in the future studies.

Experimental Section

General Experimental Methods. All reagents and starting materials were obtained from commercial suppliers and used without further purification. Anhydrous tetrahydrofuran (THF) was purified by routine procedure and distilled over sodium under nitrogen before using. The bisanthenequinone **7** was prepared according to literature.[13] Photocyclization reaction was carried out in a photochemical reactor with irradiation of a 450 W mercury-vapor lamp. Column chromatography was performed on silica gel. All chemical shifts in NMR spectra are quoted in ppm, relative to tetramethylsilane, using the residual solvent peak as a reference standard. High resolution mass spectra were recorded with EI ionization source. UV−vis absorption and fluorescence spectra were recorded in DCM solution on a spectrometer and a fluorometer, respectively. Cyclic voltammetry measurements of compounds **4−6** in DCM (1 mM) was performed with a three-electrode cell, using 0.1 M Bu_4NPF_6 as supporting electrolyte, AgCl/Ag as reference electrode, gold disk as working electrode, Pt wire as counter electrode, and scan rate at 50 mV/s. Thermogravimetric analysis (TGA) was carried out at a heating rate of 10 °C/min under nitrogen flow. Differential scanning calorimetry (DSC) was performed at a heating/cooling rate of 10 °C/min under nitrogen flow.

7,14-Bis(3,5-di-*tert*-butylphenyl)-7,14-dihydrophenanthro[1,10, 9,8-*opqra*]perylene-7,14-diol (8a). Magnesium (82 mg, 3.42 mmol) and a piece of iodine crystal were placed in dry THF

(1 mL). To the mixture was added dropwise 1-bromo-3,5-di-*tert*-butylbenzene (707 mg, 2.62 mmol) in dry THF (10 mL), and the mixture was stirred at room temperature for 2 h to generate Grignard reagent. The as-prepared Grignard reagent was transferred into a suspension of bisanthenequinone **7** (100 mg, 0.26 mmol) in dry THF (20 mL), and the mixture was stirred at room temperature overnight. The reaction was quenched with water (100 mL) and extracted with diethyl ether. The organic layer was washed by water and dried over anhydrous Na_2SO_4. After removal of solvent, the residue was further purified by column chromatography on silica gel with DCM/hexane = 2:1 (v/v) as eluent to afford **8a** (114 mg, 57%) as a light yellow solid. Mp > 300 °C. ^{1}H NMR (500 MHz, $CDCl_3$) δ 1.04 (s, 36 H), 3.22 (s, 2 H), 7.02 (d, J = 1.25 Hz, 4 H), 7.07 (t, J = 1.9 Hz, 2 H), 7.56 (dd, J = 7.86 Hz, 4 H), 7.89 (d, J = 6.3 Hz, 4 H), 8.40 (d, J = 7.55 Hz, 4 H). ^{13}C NMR (125 MHz, $CDCl_3$) δ 31.35, 34.68, 74.91, 119.25, 120.01, 120.14, 122.05, 123.81, 127.16, 127.36, 128.92, 141.36, 149.45, 149.93. EI MS: m/z = 760.6 ([M]), calculated exact mass 760.4. HR EI MS: m/z = 760.4257 ([M]), calculated exact mass for $C_{56}H_{56}O_2$ 760.4280.

7,14-Bis(3,5-di-*tert*-butylphenyl)phenanthro[1,10,9,8-*opqra*]-perylene (4). In absence of light, a mixture of **8a** (200 mg, 0.26 mmol), NaI (394 mg, 2.62 mmol), $NaH_2PO_2 \cdot H_2O$ (508 mg, 3.94 mmol), and acetic acid (50 mL) was heated to reflux for 2 h. After cooling to room temperature, the deep blue precipitate was collected by filtration, washed with water and methanol, and purified by column chromatography on silica gel with hexane/toluene = 1:1 (v/v) as eluent to afford **4** (133 mg, 70%) as a deep blue solid. Mp > 300 °C. ^{1}H NMR (500 MHz, $CDCl_3$) δ 1.41 (s, 36 H), 7.29 (d, J = 1.9 Hz, 4 H), 7.34 (dd, J = 8.2 Hz, 4 H), 7.42 (d, J = 8.8 Hz, 4 H), 7.56 (t, J = 1.58 Hz, 2 H), 8.25 (d, J = 7.55 Hz, 4 H). ^{13}C NMR (125 MHz, $CDCl_3$) δ 31.62, 35.03, 120.18, 125.51, 126.39, 126.43, 127.10, 132.36, 132.39, 151.02. EI MS: m/z = 726.5 ([M]), calculated exact mass 726.4. HR EI MS: m/z = 726.4204 ([M]), calculated exact mass for $C_{56}H_{54}$ 726.4226.

7,14-Bis(4-(trifluoromethyl)phenyl)-7,14-dihydrophenanthro-[1,10,9,8-*opqra*]perylene-7,14-diol (8b). Magnesium (95 mg, 3.94 mmol) and a piece of iodine crystal were placed in dry THF (1 mL). To the mixture was added dropwise 1-bromo-4-(trifluoromethyl)benzene (591 mg, 2.62 mmol) in dry THF (10 mL), and the mixture was stirred at room temperature overnight to generate Grignard reagent. The as-prepared Grignard reagent was transferred into a suspension of bisanthenequinone **7** (100 mg, 0.26 mmol) in dry THF (20 mL) and the mixture was stirred at room temperature overnight. The reaction was quenched with water (100 mL) and extracted with diethyl ether. The organic layer was washed by water and dried over anhydrous Na_2SO_4. After removal of solvent, the residue was purified by column chromatography on silica gel with DCM/hexane = 2:1 (v/v) as eluent to afford **8b** (103 mg, 60%) as a light yellow solid. Mp > 300 °C. ^{1}H NMR (500 MHz, $CDCl_3$) δ 3.26 (s, 2 H), 7.33 (br, 8 H), 7.59 (dd, J = 7.58 Hz, 4 H), 7.83 (d, J = 6.95 Hz, 4 H), 8.45 (d, J = 7.55 Hz, 4 H). ^{13}C NMR (125 MHz, $CDCl_3$) δ 74.09, 119.10, 122.68, 123.60, 124.87, 125.12, 125.15, 127.62, 127.77, 129.11, 140.28, 153.52. EI MS: m/z = 672.3 ([M]), calculated exact mass 672.2. HR EI MS: m/z = 672.1511 ([M]), calculated exact mass for $C_{42}H_{22}F_6O_2$ 672.1524.

7,14-Bis(4-(trifluoromethyl)phenyl)phenanthro[1,10,9,8-*opqra*]-perylene (5). In absence of light, a mixture of **8b** (100 mg, 0.15 mmol), NaI (225 mg, 1.5 mmol), $NaH_2PO_2 \cdot H_2O$ (290 mg, 2.25 mmol), and acetic acid (25 mL) was heated to reflux for 2 h. After cooling to room temperature, the deep blue precipitate was collected by filtration, washed with water and methanol, and purified by column chromatography on silica gel with hexane/toluene = 3:1 (v/v) as eluent to afford **5** (68 mg, 72%) as a deep blue solid. Mp > 300 °C. ^{1}H NMR (500 MHz, $CDCl_3$) δ 7.30 (d, J = 8.85 Hz, 4 H), 7.39 (dd, J = 7.88 Hz, 4 H), 7.40 (d, J = 8.3 Hz, 4 H), 7.92 (d, J = 8.2 Hz, 4 H), 8.29 (d, J = 7.6 Hz, 4 H).

^{13}C NMR (75 MHz, CDCl$_3$) δ 120.65, 125.85, 125.90, 126.37, 127.00, 131.77, 131.99, 132.27, 134.69, 142.90. EI MS: m/z = 638.2 ([M]), calculated exact mass 638.1. HR EI MS: m/z = 638.1469 ([M]), calculated exact mass for C$_{42}$H$_{20}$F$_6$ 638.1469.

7,14-Bis(triisopropylsilylethynyl)phenanthro[1,10,9,8-*opqra*]-perylene (6). To a solution of triisopropylsilylacetylene (479 mg, 2.629 mmol) in anhydrous THF (30 mL) at 0 °C was added dropwise *n*-BuLi (1.6 M in hexanes, 1.56 mL, 2.5 mmol). The solution was allowed to stir for 30 min at 0 °C before bisanthenequinone **7** (100 mg, 0.26 mmol) was added in one portion. The mixture was warmed to room temperature, stirred overnight, and then poured into a large amount of water. The mixture was extracted with chloroform, and the organic layer was washed with brine and dried over MgSO$_4$. The solvent was removed by evaporation and the residue was dried under vacuum. In absence of light, a mixture of the crude product diol **8c** (218 mg, 0.26 mmol), NaI (394 mg, 2.62 mmol), NaH$_2$PO$_2$·H$_2$O (406 mg, 3.15 mmol) and acetic acid (10 mL) was heated to reflux for 2 h. After cooling to room temperature, the deep green precipitate was collected by filtration, washed with water and methanol, and purified by column chromatography on silica gel with hexane/toluene = 3:1 (v/v) as eluent to afford **6** (68 mg, 72%) as a deep green solid. Mp > 300 °C. ^{1}H NMR (500 MHz, CDCl$_3$) δ 1.32 (br, 6 H, isopropyl), 1.33 (br, 36 H, isopropyl), 7.42 (br, 4 H), 7.95 (br, 4 H), 8.19 (br, 4 H). EI MS: m/z = 710.5 ([M]), calculated exact mass 710.4. HR EI MS: m/z = 710.3756 ([M]), calculated exact mass for C$_{50}$H$_{54}$Si$_2$ 710.3764.

Supporting Information Available: Original characterization spectra of all new compounds, photostability test of **4**−**6** under irradiation of UV lamp, chemical oxidation titration process of **4**−**6** by iodine, and DFT calculation details. This material is available free of charge via the Internet at http://pubs.acs.org.